Dependence of Electrochemical Properties of Vanadium Oxide Films on Their Nano- and Microstructures

Kyoungho Lee,*,†,‡ Ying Wang,† and Guozhong Cao†

Materials Science and Engineering, University of Washington, 302 Roberts Hall, Box 352120, Seattle, Washington 98195, and Materials Science and Engineering, Soonchunhyang University, 646, Eupnae-Ri, Shinchan-Myun, Asan-Si, Chungnam, Korea

Received: April 2, 2005; In Final Form: June 26, 2005

Platelet- and fibrillar-structured V_2O_5 films have been prepared by solution methods, and their electrochemical Li^+ intercalation properties have been studied. Platelet film consists of 20−30 nm sized V_2O_5 particles with random orientation, whereas fibrillar film is comprised of randomly oriented fibers though most of them protrude from the substrate surface. These platelet- and fibrillar-structured films exhibit relatively larger surface area and shorter diffusion path for Li^+ intercalation than plain thin film structure. The processing methods, the discharge capacity, and cyclic performance of these films are compared with those of the conventional plain structured film.

Introduction

Vanadium pentoxide (V_2O_5) has attracted a lot of attention as a Li intercalation host, due to its layered structure and, hence, the ability to intercalate ions or molecules between the adjacent layers.[1,2] Electrical energy is stored in the form of a chemical potential during deintercalation, and this chemical energy is released in the form of electricity during intercalation. This interesting electrochemical performance has created significant interest in V_2O_5 for various applications such as a cathode for high energy density lithium batteries,[3,4] as an electrode material for electrochemical pseudocapacitors,[5,6] and for electrochromic devices[7] and electrooptic switches.[8]

In energy storage applications, the fundamental advantage of intercalation-based high rate systems as compared to other non-Faradic reaction-based electrochemical systems is that the former are characterized by three-dimensional energy storage and release processes, whereby the intercalate moves into the host solid phase. This three-dimensional system possesses a significant advantage over conventional electrochemical capacitors which are inherently two-dimensional. The energy that can be stored in a three-dimensional electrode structure is much larger than that stored in conventional capacitors, but the depth of penetration by intercalation is limited by diffusion. Previous study indicated that the diffusion coefficient of Li^+ in crystalline V_2O_5 is inherently low, i.e., $D = \sim 10^{-12}$ cm^2/s.[9] Considering this inherently low diffusion rate of Li^+ in V_2O_5, many researchers found that the capacity of lithium intercalation at high discharge rates can be improved by controlling the size and shape of the individual particles and the morphology of the V_2O_5 electrode film. For example, the rate capabilities of the nanostructured electrodes (e.g., an assembly of tubular or fibrillar particles of the electrode material which protrude from the surface of the current collector like the bristles of a brush) were compared with the rate capabilities of thin-film electrodes containing the same type and quantity of the electrode material, and galvanostatic discharge experiments showed that the nanostructured electrode delivered higher capacities than the thin-film electrodes.[10−13] This is because for the microstructured electrode, the Li^+ diffusion distances are shorter and the surface areas are larger. The preparation of nanostructured electrodes, however, mainly relies on the template-based growth methods. The advantages of template-based growth methods are the ability of fabricating unidirectionally aligned and uniformly sized nanorod arrays of a variety of electrode materials. However, such methods suffer from inherent limitations, such as post-heat-treatment required to pyrolyze polymeric membranes prevents the usage of low-temperature phase or incomplete removal of template material through chemical etching.

In this paper, we report a simple growth method for either fibrillar- or platelet-structured electrode film which possesses a high surface area and a short path for Li^+ diffusion. Li intercalation properties in platelet-, fibrillar- and plain-structured vanadium oxide films are studied, and the dependence of electrochemical properties including fatigue resistance on nano- and microstructures is discussed.

Experimental Section

(1) Preparation of Samples. Vanadium pentoxide films having three different morphologies were prepared. Figure 1 shows the fabricated V_2O_5 films with different surface morphologies. These V_2O_5 thin films with different morphologies were prepared using different starting materials. As shown in Figure 1a, the conventional plain vanadium pentoxide film was prepared from the vanadium sol method as reported by Fontenot el al.[14] In this approach, a V_2O_5 powder (99.8%, Alfa Aesar) was first dissolved in iced-cooled 30 wt % H_2O_2 (J.T. Baker) aqueous solution with a V_2O_5 concentration of 0.15 mol/L. After the mixture was stirred for 1.5 h at room temperature, the excess H_2O_2 was decomposed by sonication, and a red-brown gel was obtained. The resultant gel was then redispersed in deionized water producing a sol that has a red-brownish color, contains 0.01 mol/L vanadium ions, and has a pH of 2.7. Hereafter this method will be designated as the "method A".

* Corresponding author. E-mail: khlee@sch.ac.kr.
† University of Washington.
‡ Soonchunhyang University.

10.1021/jp051686q CCC: $30.25
Published on Web 08/11/2005

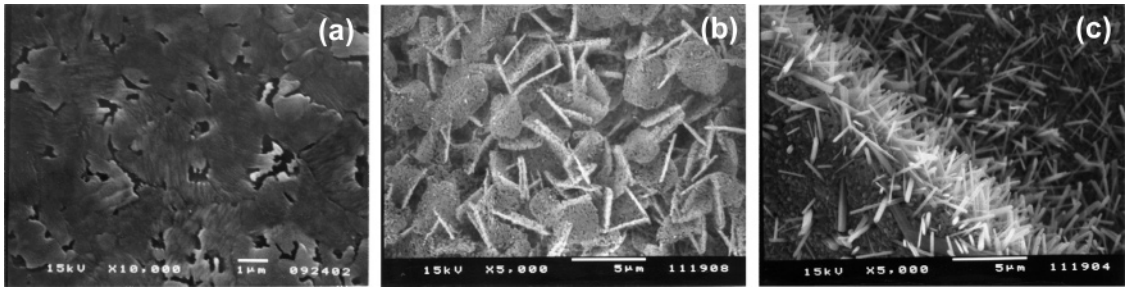

Figure 1. SEM micrographs of as-prepared V_2O_5 thin films: (a) plain structured film; (b) in situ grown platelet structured film; (c) in situ grown fibrillar structured film.

The platelet structured film shown in Figure 1b was prepared from the solution containing VO^{2+} ions. The V_2O_5 powder (99.8%, Alfa Aesar) was first dissolved in iced cooled 30 wt % H_2O_2 (J.T. Baker) aqueous solution and 45 wt % HCl (J.T. Baker) with a V_2O_5 concentration of 0.15 mol/L. After the mixture was stirred for 1.5 h at room temperature, the excess H_2O_2 was decomposed by sonication, and a red-brown gel was obtained. After that, the obtained gel was dissolved by adding 2 M H_2SO_4 (96.5%, Fisher). After the mixture was stirred for 24 h at room temperature, the obtained solution is yellowish green and contains 0.01 mol/L vanadium ions and has a pH of 1.20. Hereafter this method will be designated as the "method B".

The fibrillar particle precipitated film as shown in Figure 1c was also prepared from the vanadium solution but using different starting chemicals. The chemicals used in making solution were $VOSO_4 \cdot nH_2O$ (Alfa Aesar) and H_2SO_4 (96.5%, Fisher). A 0.01 mol/L VO^{2+} solution was prepared by dissolving $VOSO_4 \cdot nH_2O$ into deionized water together with H_2SO_4. Such solution has a blue color and a pH of 1.5. Hereafter this method will be designated as the "method C".

Without further adjustment of the pH values of the individual sol and solution, the films were subsequently made by coating the individual sol or solution onto Ti foil, followed by drying at 60 °C for 1 h and firing at 500 °C for 1 h in air.

(2) Sample Characterizations. Scanning electron microscopy (SEM, JEOL JSM-5200) was used to examine the different morphologies of the coated vanadium pentoxide films heat treated at 500 °C for 1 h. The developed phase and the preferred orientation of the developed phase in the coated films were analyzed by X-ray diffraction (XRD) using a Phillips PW1830 diffractometer with Cu Kα radiation operated at 40 kV and 20 mA.

The effects of different morphology on the electrochemical properties of V_2O_5 films were investigated by using a three-electrode cell with a platinum counter electrode and a silver wire in the 0.1 mol/L $AgNO_3$ solution as the reference electrode. A 1 mol/L solution of lithium perchlorate (99.99%, Aldrich) in propylene carbonate (99.7%, Aldrich) was used as the electrolyte. The chronopotentiometric measurement was carried out using a CHI605B potentiostat/galvanostat (CHI instrument). The cutoff voltage was −1.5 and 0.5 V (vs Ag/Ag^+) under the current density of 0.27 A/g (i.e., 0.8 C rate).

Results and Discussion

Figure 1 shows the SEM observation of the surface morphology of the resulting films. The V_2O_5 film made from method A (see Figure 1a) shows a typical smooth surface morphology with some voids throughout the film. The film prepared by using method B (see Figure 1b) shows a randomly oriented platelet-like morphology with most platelets standing almost vertically and commonly having a thickness of 20−30 nm. Figure 1c shows the film prepared using method C, and the film shows an assembly of fibrillar particles of 20−40 nm in diameter protruding from the current collector surface like the bristles of a brush. Sol−gel route vanadium pentoxide thin films have been fabricated by many researchers, and the surface morphology shown in Figure 1a is the typical morphology which can be found in other reports.[3,4] Several papers reported V_2O_5 films consisting of a needlelike structure;[15,16] however, needlelike or fibrillar V_2O_5 particles typically lay parallel to the substrate surface. Both platelet- and fibrillar-structured films are unique and perpendicularly standing platelets and fibrils offer readily accessible high surface area and relatively short, straight, and simple path for Li^+ diffusion than the plain films consisting of parallel-stacking platelet particles.

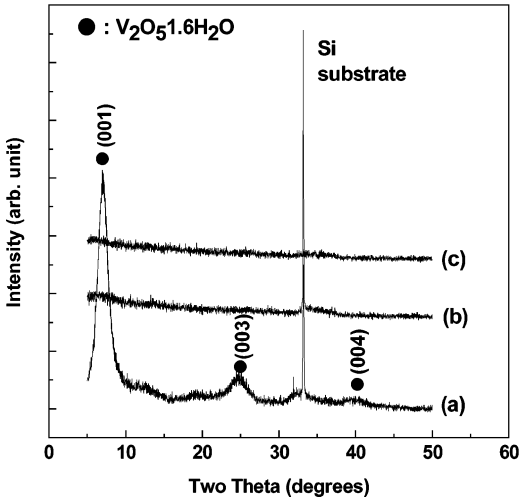

Figure 2. X-ray diffraction patterns of dried films at 60 °C for 1 h. The films are prepared from (a) method A, (b) method B, and (c) method C.

The growth mechanisms of these fibrillar- or platelet-structured films are not known, but some possibilities are discussed below. Figure 2 shows the X-ray diffraction spectra of the films after being dried at 60 °C for 1 h. After drying, the film made from the method A shows highly textured hydrated vanadium pentoxide ($V_2O_5 \cdot 1.6H_2O$) with [001] perpendicular to the substrate surface. Vigolo et al.[17] established a phase diagram of stable vanadium species as a function of the concentration of vanadium ions and the pH. According to this diagram, the prepared solution (colloidal dispersion) with 0.01 M vanadium ions and a pH of 2.7 consists of stable hydrated V_2O_5 ribbon clusters. The smooth surface morphology resulted from these platelet particles of the layer structured hydrate vanadium oxide aligned parallel to the substrate surface during the coating. Subsequent dehydration during heat treatment at 500 °C resulted in little change in surface morphology. The films prepared from the vanadium solutions (methods B and

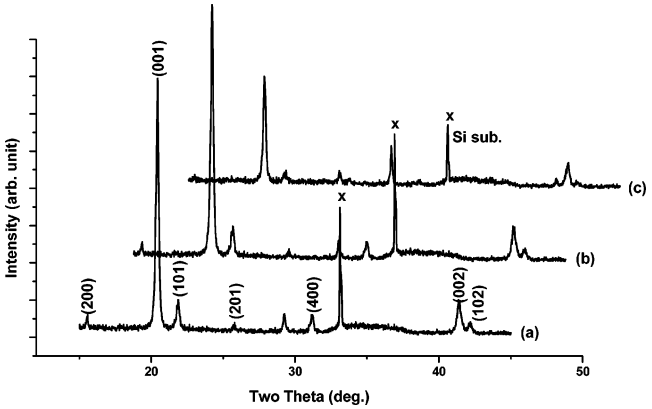

Figure 3. X-ray diffraction patterns of V_2O_5 films after firing at 500 °C for 1 h: (a) plain structured film; (b) platelet structured film; (c) fibrillar structured film.

C) show no crystalline phase after drying and are likely to be amorphous. The similar platelet- or fibrillar-structured films have been reported in the literature; they were found to be formed by poisoning effect from sputtering target and the grains dropped onto the film surface during formation of the virgin film.[18] However, our results have shown that the formation of fibrillar- or plate-structured film occurs in the heat treatment and is not due to anything in the source of sol or gel. SEM observation has showed that the dried film has no sign of the formations of platelet or fibrillar grains. Therefore, it is believed that the platelet or fibrillar structures are likely developed during the subsequent heat treatment at 500 °C. Crystallization from amorphous occurs more easily at surface or interface. In the present study, it is possible that the crystallization started at the surface of amorphous films. Since both fibrillar and platelet shapes are common morphology of vanadium pentoxide particles, it is easy to form platelets and fibrils from an amorphous with the growth direction perpendicular to the amorphous films surface, resulting in protruding platelets and fibrils. It is also well-known that the growth mechanism of a crystal phase from the amorphous state depends on the interfacial energy between the growing phase and the matrix. The vanadium solutions prepared from methods B and C have different starting vanadium-containing chemicals. Therefore, the obtained dried amorphous films from the solutions may have different surface energy and this may be attributed to have different morphologies of V_2O_5 films.

Figure 3 shows the X-ray diffraction spectra of the films fired at 500 °C for 1 h. All X-ray spectra demonstrated a large deviation in relative peak intensity from the standard pattern of orthorhombic V_2O_5 powder. There was a strong preferential orientation along the [001] direction, which is in good agreement with the literature.[16] In particular, the film made from method A showed the most preferred orientation along the *c* axis. This resulted from the platelet particles of the layer structured hydrate vanadium oxide formed during sol processing prior to coating. Coating aligns the platelet particles parallel on the substrate surface. Heat treatment at 500 °C is unlikely to change the crystal orientation. Even though there is slight difference in degree of preferred orientation, vanadium pentoxide (V_2O_5) is the only crystalline phase developed in three different films after heat treating at 500 °C for 1 h.

Figure 4a compares the initial discharge capacities of the V_2O_5 films with various preparation methods under a constant current density of 0.27 A/g. All chronopotentiometric curves show a typical discharge curve of crystalline V_2O_5 with a stepwise shape due to the phase change of $Li_xV_2O_5$ during Li^+ intercalation.[12,18]

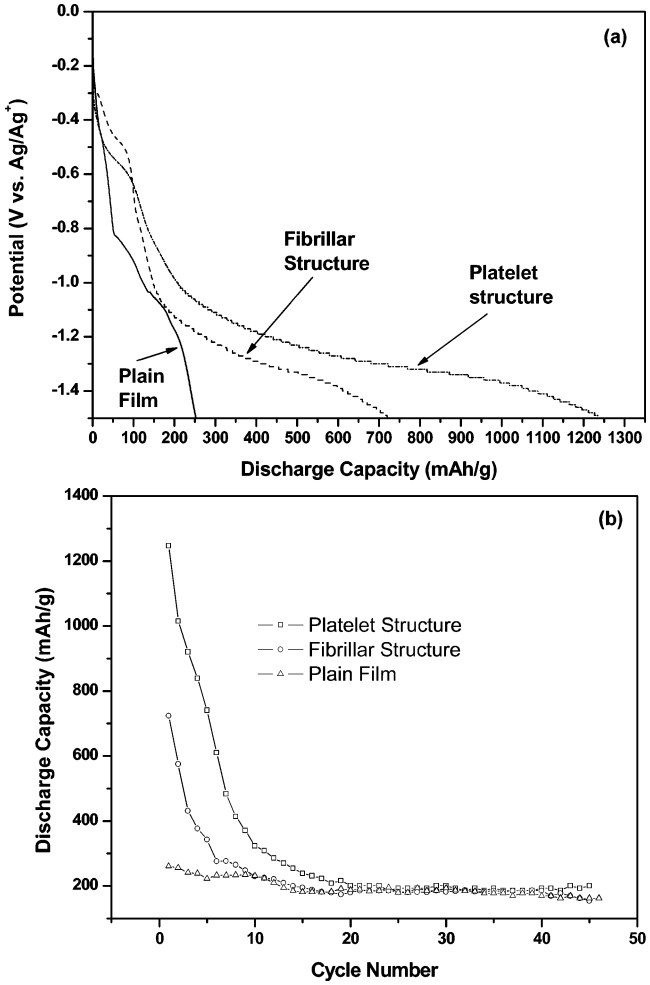

Figure 4. The performance of Li^+ intercalation of V_2O_5 films with various surface morphologies: (a) the initial discharge capacities at constant current density of 0.27 A/g; (b) cyclic performance.

The film with platelet structure shows the highest initial discharge capacity, and the plain thin film shows the lowest initial discharge capacity. This result may arise due to the argest intercalation surface and the shortest diffusion distance of the platelet-structured film. It is well-known that the particle size and the surface area of the electrode dramatically affect the intercalation rate and capacity because diffusion of Li^+ within the electrode material is slower and more difficult than in a liquid electrolyte or along the grain boundaries. Therefore, a short diffusion distance due to the small particle size will prevent concentration polarization of Li^+ within the electrode, allowing the retention of cell voltage which results in delaying termination of the discharge up to the maximum capacity of the material. A high surface area due to small particle size can reduce the Li^+ insertion rate density per unit area during the discharging process. This reduced insertion rate also delays the capacity loss associated with concentration polarization to higher discharge current density. The initial discharge capacities of the platelet and the fibrillar structured films are 1240 and 720 mA h/g, respectively. These values are relatively higher than the previously reported values. It is believed that the original large discharge capacities may arise from lack of the interlayered cross-linking.[19] Figure 4b shows cyclic performance of the films. Unfortunately, the capacities of both platelet and the fibrillar structured films decay very fast initially with cycling tests. After 20 cycles, all three films exhibit almost the same discharge capacities. The plain structured film retains nearly 70% of its

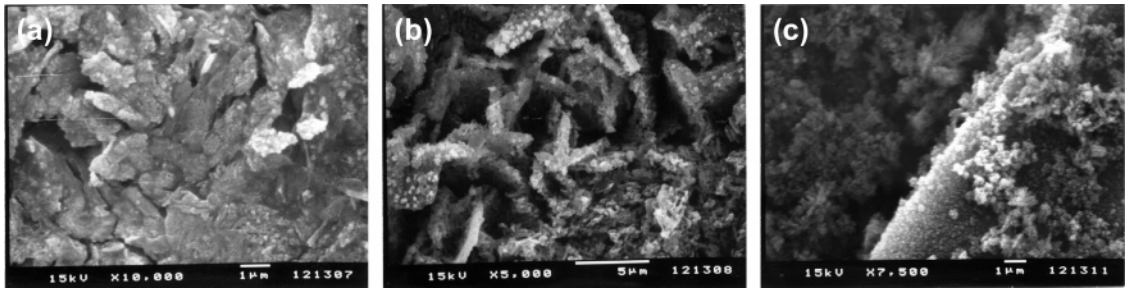

Figure 5. SEM micrographs of V_2O_5 thin films showing after cyclic test: (a) plain structured film; (b) platelet-structured film; (c) fibrillar structured film.

initial discharge capacity after 45 cycles. However, platelet and fibrillar structured films retain only 16% and 22% of their respective initial discharge capacities. This poor cyclic performance of platelet and fibrillar structured V_2O_5 films is likely due to the degradation of each platelet or fibril.

The surface morphologies of the films after cyclic tests are shown in Figure 5. Figure 5a shows the surface morphology of plain film after cyclic test. The film remains in a good condition (compare Figure 1a) though there might be traces of $LiClO_4$ crystals covering the surface. However, the surfaces of platelet and fibrillar structured films show an appreciable change after cyclic tests and become similar to the plain films. Since platelet and fibrillar structured films have large initial Li^+ intercalation capabilities, a structural breakdown during electrochemical intercalation is more likely to lead to electrochemical failure. It is reasonable that as the distinction of nano- and microstructures in three films gradually vanishes as the cyclic number increases, the electrochemical intercalation properties of three films becomes almost identical. Improvement of the stability of platelet and fibrillar nanostructures is an obvious challenge. Addition of secondary phase, such as TiO_2, to vanadium oxide to form a composite has been proven to be an efficient approach to enhance the cyclic fatigue resistance with enhanced mechanical integrity.[21−23] Similar concepts would be applicable to the platelet and fibrillar nanostructured vanadium oxide films.

It is not known why the platelet and fibrillar films have such high initial capacities (1240 and 720 mA h/g, respectively), though some possible reasons are briefly discussed in the following. The presence of a trace amount of sulfur from the precursor may exert some kind catalytic influences on Li ion intercalation in vanadium pentoxide, and this hypothesis is being verified in our group. Another possible reason is that the high surface area derived from the fine microstructures may contribute a significant amount of surface charge, resulting in an extremely high apparent capacity.[24] This may also explain the degradation of capacity of both platelet and fibrillar films as the cyclic number increases, since fine microstructure collapses and surface area decreases. It is also surprising to see the capacities of both platelet and fibrillar films degrade rapidly with the first 10 cyclic tests, while the plain film almost retains its initial capacity. It is known that active materials with nano- or submicrometer-sized structures are less subject to subdivision because both the absolute volumetric changes and the effective mechanical stresses are reduced within the particles.[25,26] However, the opposite might be true when the fine structures are loosely adhered to each other. Small volumetric change of individual fine structures may result in disintegration or collapse of the overall structure; this may be the case in the present study. A few more experiments are underway in our lab to verify the influences of possible sulfur contamination on Li intercalation and the structure stability when subjected to cyclic tests.

Conclusions

Platelet- and fibrillar-structured V_2O_5 films have been prepared by solution methods, and the discharge capacities and cyclic performance of these films were compared with the conventional plain structured film. The initial discharge capacities of platelet- and fibrillar-structured V_2O_5 films are 1240 and 720 mA h/g, respectively, which are far larger than the initial discharge value (260 mA h/g) of the plain structure film. Such large discharge capacity values are ascribed to the combined effects of reduced Li^+ diffusion distance, which prevents concentration polarization of Li^+ in V_2O_5 electrode, and poor interlayered cross-linking offering more Li^+ intercalation. However, platelet- and fibrillar-structured V_2O_5 films were easily degraded during electrochemical cyclic tests.

Acknowledgment. This work was supported by Ministry of Commerce, Industry and Energy Republic of Korea (MOCIE) through the BIT Wireless Communication Devices Research Center at Soonchunhyang University

References and Notes

(1) Whittingham, M. S. *J. Electrochem. Soc.* **1976**, *123*, 315.
(2) Bachmann, H. G.; Ahmend, F. R.; Barnes, W. H. *Z. Kristallogr.* **1961**, *115*, 110.
(3) Park, H. K.; Smryl, W. H.; Ward, M. D. *J. Electrochem. Soc.* **1995**, *142*, 15.
(4) Swider-Lyons, K. E.; Love, C. T.; Rolison, D. R. *Solid State Ionics* **2002**, *152−153*, 99.
(5) Shimizu, A.; Tsumura, T.; Inagaki, M. *Solid State Ionics* **1993**, *63−65*, 479.
(6) Portion, E.; Salle, A. L. G. A.; Verbaere, A.; Piffard, Y.; Guyomard, D. *Electrochim. Acta* **1999**, *45*, 197.
(7) Cogan, S. F.; Nguyen, N. M.; Perrotti, S. J.; Rauh, R. D. *J. Appl. Phys.* **1989**, *60−2*, 749.
(8) Nadkarni, G. S.; Shirodkar, V. S. *Thin Solid Films* **1983**, *105*, 115.
(9) Watanabe, T.; Ikeda, Y.; Ono, T.; Hibino, M.; Hosoda, M.; Sakai, K.; Kudo, T. *Solid State Ionics* **2002**, *151*, 313.
(10) Che, G.; Jirage, K. B.; Fisher, E. R.; Martin, C. R. *J. Electrochem. Soc.* **1997**, *144*, 4296.
(11) Nishizawa, M.; Mukai, K.; Kuwabata, S.; Martin, C. R.; Yoneyama, H. Livage, *J. Electrochem. Soc.* **1997**, *144*, 1923.
(12) Patrissi, C. J.; Martin, C. R. *J. Electrochem, Soc.* **1999**, *146*, 3176.
(13) Takahashi, K.; Limmer, S. J.; Wang, Y.; Cao, G. Z. *J. Phys. Chem. B* **2004**, *108*, 9795.
(14) Fontenot, C. J.; Wiench, J. W.; Pruski, M.; Schrader, G. L. *J. Phys. Chem. B* **2000**, *104*, 11622.
(15) Kumagai, N.; Kitamoto, H.; Baba, M.; Durand-Vidal, S.; Devilliers, D.; Groult, H. *J. Appl. Electrochem.* **1998**, *28*, 41.
(16) Fang, G. J.; Liu, Z. L.; Wang, Y.; Liu, Y. H.; Yao, K. L. *J. Vac. Sci. Technol., A* **2001**, *19*, 887.
(17) Vigolo, B.; Zakri, C.; Nallet, F.; Livage, J.; Coulon, C. *Langmuir* **2002**, *18*, 9121.
(18) Nam, S.; Lim, Y. C.; Park, H. Y.; Jeon, E. J.; Yoon, Y. S.; Cho, W.; Cho, B. W.; Yun, K. S. *Korean J. Chem. Eng.* **2001,** *18*, 673.
(19) Lantelme, F.; Mantoux, A.; Groult, H.; Lincot, D. *J. Electrochem. Soc.* **2003**, *150*, A1202.
(20) Wang, J.; Curtis, C. J.; Schulz, D. L.; Zhang, J. G. *J. Electrochem. Soc.* **2004**, *151*, A1.

(21) Minett, M. G.; Owen, J. R. *J. Power Sources* **1990**, *32*, 81.
(22) Davies, A.; Hobson, R. J.; Hudson, M. J.; Macklin, W. J.; Neat, R. J. *J. Mater. Chem.* **1996**, *6*, 49.
(23) Özer, N.; Sabuncu, S.; Cronin, J. *Thin Solid Films* **1999**, *338*, 201.
(24) Béguin, F.; Chevallier, F.; Vix, C.; Saadallah, S.; Rouzaud, J. N.; Frackowiak E. *J. Phys. Chem. Solids* **2004**, *65*, 211.
(25) Maranchi, J. P.; Velikokhatnyi, O. I.; Datta, M. K.; Kim, I.; Kumta, P. N. Ceramic Materials for Lithium-Ion Battery Applications. In *Chemical Processing of Ceramics*, 2nd ed.; Lee, B., Komarneni, S., Eds.; CRC: Boca Ratan, in press.
(26) Winter, M.; Besenhar, J. O.; Spahr, M. E.; Novμk P. *Adv. Mater*. **1998**, *10*, 725.